High-Temperature Measurement System with Wireless Electronics for Harsh Environments

E. Sardini, M. Serpelloni
Department of Information Engineering
University of Brescia
Via Branze 38, 25123 Brescia, Italy
mauro.serpelloni@ing.unibs.it

Abstract— **High temperature measurement systems do not allow the use of traditional measurement techniques. In the presence of high temperatures the proper functioning of electronics is compromised. Furthermore, if the measurement environment is also hermetic, the traditional cabled measurement technique cannot be adopted. In this article a system to measure the temperature up to 330 °C for harsh environments is proposed. The system is based on a hybrid MEMS placed inside the measuring chamber constituted solely by passive components (an inductor connected to a planar micromachined variable capacitor) and an external reading unit, located in the safe environment. The hybrid MEMS was designed and characterized, as well as the electronics of the readout unit. The results obtained and reported in the article are quite good with those measured by a reference instrument. The complete measurement system is presented as a viable solution to the measurement of high temperatures in harsh industrial environments.**

Keywords; Autonomous sensor; contactless telemetric system; high-temperature measurement; microelectromechanical systems (MEMS); wireless system.

I. INTRODUCTION

In industrial environments, high temperature measurements are required for process control, safety evaluation, reliability prediction, product liability, and quality control. Since the measurement environment is harsh, it is insulated from the external side where the control or processing electronics is placed. In several applications furthermore, the environment must be hermetic as well, such as in controlled drying processes and pressurized fluids. In these cases, the environment is commonly unsuitable for electronic active circuits since they do not work in presence of temperatures greater than 100 °C thus excluding the possibility of using commonly known wireless sensor network. Moreover most existing temperature sensors cannot be used since they require a cabled solution. The solution is to measure high-temperatures without contact. In contactless techniques the sensing element is positioned in the harsh environment, while the second part of the measurement system, consisting of the active devices of the conditioning electronics required to extract the measurement information, is outside in a safe zone. In the literature, several examples of contactless measurements are reported using optical sensors [1-4]. Optical instruments such as pyrometers or infrared optical sensors sometimes offer a solution. In [3], an infrared temperature measurement system able to measure between 500 °C and 1300 °C is described. In [4], the authors propose the use of microwave radiometric to noninvasively measure and control the temperature during the microwave sintering processes. A different measurement approach is described in [5], the authors present a contactless magnetic measurement solution: NiFe sensors, whose properties are very sensitive to temperature, are associated to remote magnetic transducers: the active part is placed outside. In [6] SAW (Surface Acoustic Wave) sensors for high-temperature applications are analyzed highlighting the material issues: the high-temperature characteristics of novel devices are investigated by finite-element simulation and by experimental deformation analysis. Assembly, interconnection, and packaging techniques are also discussed. In [7] materials and packaging solution for microsensors, systems, and devices for high-temperature and harsh-environment are analyzed and compared. Among the contactless systems, autonomous sensors are an interesting solution for connecting the probe positioned in the hazardous zone with the conditioning electronics in the safe zone. They represent a viable solution when the measurement environment is contained in an enclosed and hermetic space and the required wire-link through the separating wall, between the harsh and safe zones, is not possible due to the presence of high pressure or to the use of expensive connecting techniques. Usually sensing techniques are based on a change of the resonant frequency of a LC circuit. In the literature, examples of such systems are reported in [8-12]. In [12] a passive wireless temperature sensor operating in harsh environment for high-temperature (up to 235 °C) rotating component monitoring is reported. Contactless measurement techniques require also the use of special electronic systems. Several of these are based on frequency analysis or on impedance variation. In the literature different proposals are reported in order to design ad-hoc instruments for the applications. The design of electronic circuits for impedance analysis and scanning frequency can be developed in different ways, with a FPGA (Field Programmable Gate Array) approach [13-14] or with an impedance analyzer [15-16]. In [16], the impedance measurement instrumentation is based on the measurement of the real and imaginary part of impedance, working in the frequency from 10 to 100 kHz. In [17] the authors describe an impedance gain-phase analyzer; the instrument operates in the frequency range of 10 Hz to 200 kHz. In this paper, a novel temperature measurement system composed by a hybrid MEMS (Micro Electro-Mechanical Systems) [18], and the contactless front-end electronic is described. The system measures high-temperature in harsh

978-1-4244-8064-7/11/$26.00 ©2011 IEEE

industrial environments. The hybrid MEMS is composed by a planar inductor developed in thick film technology and a micromachined variable capacitor temperature sensitive [19]. The electronic circuits use telemetric technique. The system has been designed, implemented and tested. The electronics is based on a measurement technique [18] called 3-Resonances method. The distance between sensor and reader can be constant if the telemetric system is fixed with measuring chamber; otherwise the measurement system consists of the sensor placed in the oven and a mobile unit outside. The proposed system is capable of operating in both situations. To experimentally verify the characteristics of the proposed measurement system, a temperature-controlled measurement oven has been developed.

II. Description of the Temperature Measurement System

The proposed telemetric system is shown schematically in Figure 1: on the left the hybrid MEMS is placed into the harsh environment, while, on the right, the readout unit is in the safe zone. A wall separates the two zones and the two subsystems communicate through an inductive coupling. This wall must be composed of non-magnetic and non-conductive material so that guarantees the magnetic coupling.

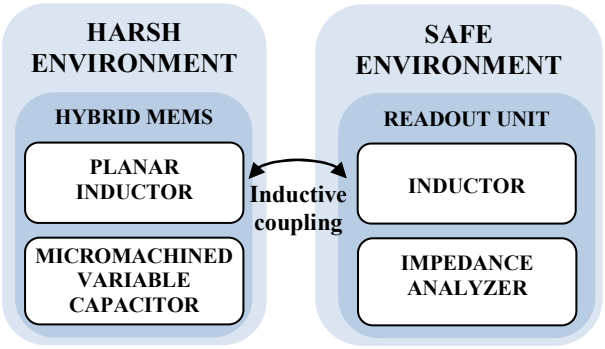

Fig. 1. Block diagram of the telemetric system.

A. Hybrid MEMS

The proposed hybrid MEMS placed in the harsh environment is composed by a microfabricated, temperature-sensitive variable capacitor fabricated using the MetalMUMPs process [19] and a planar inductor with high-temperature characteristics developed in thick film process. The layout of the variable capacitor is organized in 36 cells having capacitive behavior and connected in parallel. The single cell is based on a cascade of three bent beam structures. The interdigitated capacitor is made by two structures; the thermal expansion generates a relative movement of one structure to the second, varying the capacitance. The maximum operating temperature is limited by the maximum operating limit of nickel (350 °C). The planar inductor is obtained using thick-film technology by screen printing and micro-cutting by a laser. During the screen printing two conductive (QM14 commercialized by Du Pont) films, one overlapping the other, were deposited to reach a thickness of about 20 µm over an alumina substrate (50 mm x 50 mm x 0.63 mm). The conductive film has a resistivity of about 1.5-2.5 mΩ/sq. The deposited film was dried for 10-15 minutes at 150 °C and then was fired in a conveyor furnace for 30 minutes with a peak temperature of 850 °C. The micro-cutting process consists of material ablation by a laser. The inductors have the external diameter of 50 mm, 120 windings each of about 89 µm width and spaced 75 µm from the others. The Die is fixed to the planar inductor by a high-temperature ceramic adhesive (Resbond 931C) commercialized by Cotronics. The contact pads are bonded to the inductor terminals. The mass of the hybrid MEMS is about 8 g: 6 g (alumina), 0.2 g (Die) and the remaining mass is due to the glue.

B. Telemetric Model

An inductor, labeled readout inductor, is placed close to the hybrid MEMS, but outside in the safe environment: the two inductors constitute the telemetric coupled system. The readout inductor is directly connected to the conditioning electronics. The readout inductor is a planar spiral fabricated in thick-film technology and it has 30 windings, each of 250 µm width and spaced 250 µm from the others. The external diameter is 50 mm wide. The readout inductor and the hybrid MEMS was modeled as reported in Figure 2. R_1, R_2 are the equivalent resistances of readout and sensor; C_1, C_2 are the parasitic capacitances of the readout inductor and planar inductor, while C_S is the capacitance of the variable capacitor; L_R, L_S are the readout and sensor leakage inductances; L_M is referred to coupled flux; N_1 and N_2 are the equivalent number of the inductor windings; C_C is the coupling capacitance. Due to the geometry of the system the coupling capacitance C_C can be neglected. Whereas the working frequency range is high, the resistances R_1, R_2 can be neglected, since they have impedances of much less value than those of the series inductor L_R, L_S. L and C are L_S and C'$_S$ as seen from the primary of the ideal transformer and parameter "n" is the ratio between N_1 and N_2. C'$_S$ is the parallel of C_2 and C_S.

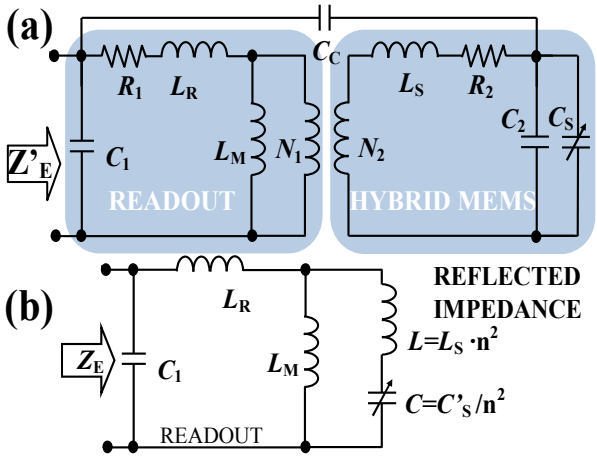

Fig. 2. (a) Telemetric inductive model in (b) simplified model.

C. Conditioning Electronics

In this section the proposed conditioning electronics for impedance measurement is presented. The impedance analyzer is composed of synthesizer for the generation of the reference signals, an analyzer of the real and imaginary part of the admittance and a controller composed of microcontroller and digital analog converter (DAC). A schematic of the proposed circuit is shown in Figure 3.

1) Synthesizer

The synthesizer consists of a DDS (Direct Digital Synthesizer), commercialized by Analog Device (AD9954). This device generates two signals, the first one is the in-phase signal (labeled as I in Figure 3), and it's used to drive the telemetric system and to extract the real part of Y'_E admittance. The second signal is the quadrature signal, (labeled as Q in the Figure 3) used for extract the imaginary part of Y'_E.

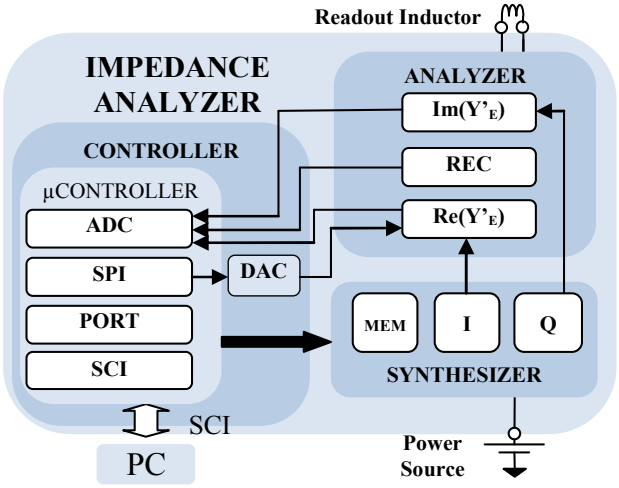

Fig. 3. Block diagram of the conditioning electronics.

2) Analyzer

The block diagram of the analyzer is show in Figure 6. The system contains three analog multipliers (Intersil HA2556), each of four quadrant type and two passive low-pass filters. The function of the circuit is to extract the real and imaginary admittance components, and identify the resonant frequencies for the measuring technique. A sinusoidal voltage, whose amplitude and frequency are respectively regulated by V_{DAC} and I, is applied to the telemetric system. The injected current is successively sent to the M_2 multiplier since the other input of the multiplier is again the in phase signal (I). The output of the Low Pass filter is the real component of the voltage that is successively acquired by ADC (Analog Digital Converter), and further processed by microcontroller. Similarly also the Imaginary component has been obtained by multiplying the voltage of the telemetric system with the Q signal. After the multiplication and the low-pass filter, the imaginary component is sampled by the ADC converter.

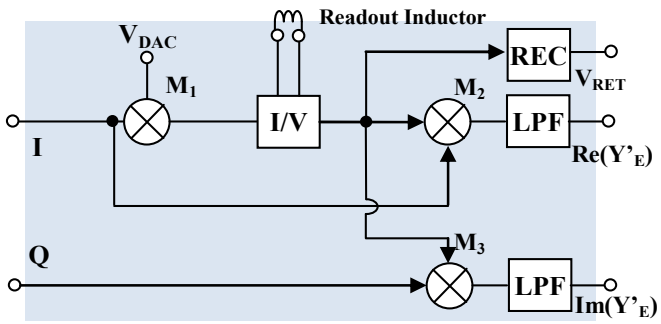

Fig. 4. Block diagram of the analyzer.

3) Controller

The controller is composed by a microcontroller, commercialized by Freescale (MCF51AC256), and a DAC. The microcontroller integrates the SPI (Serial Peripheral Interface) and SCI (Serial Communication Interface) and at least three channels of 10 bit ADC. The ADC samples the real ($Re(Y'_E)$) imaginary ($Im(Y'_E)$) and peak (REC) of the telemetric voltage. The REC signal is the output of a full bridge diode Schottky and is used by the microcontroller to regulate the amplitude of the injecting current into the telemetric system. The aim is to avoid the saturation of the multiplier since the impedance module of the telemetric system has a wide dynamic. The microcontroller program the synthesizer in order to sweep the frequency from 1 MHz to 10 MHz, during this phase the microcontroller stores the sampled data into its internal memory, and when the sweep has finished, starts the data processing. The number of samples acquired during measurement is a number settable by user. After this process, the microcontroller send the data to Personal Computer (PC) through the Serial Communication Interface (SCI), the PC analyzes the module and the phase of impedance extracting the frequencies of interest required by the 3-Resonances method.

III. MEASUREMENT TECHNIQUE

Referring to the circuit shown in Figure 2, Z_E is equal to:

$$Z_E=\frac{s^3(L_M LC+L_R C(L_M+L))+s(L_M+L_R)}{s^4 C_1(L_M LC+L_R C(L_M+L))+s^2(C_1(L_M+L_R)+C(L_M+L))+1} \quad (1)$$

The impedance reported in (1) has three resonant frequencies. First (f_{ra}) and second resonant frequency (f_{rb}) both influenced by C_1 and C. The resonant frequency (f_a) is influenced only by C and it is more sensitive to C than the other two frequencies. Its expression is:

$$f_a=\frac{1}{2\pi\sqrt{C\left(L+\frac{L_M L_R}{L_R+L_M}\right)}} \quad (2)$$

f_a depends on C, and also on distance, since the distance changes the coupled and leakage flux modifying the value of L_M, L_R. The other two frequencies (f_{ra} and f_{rb}) have dependence more complex and dependent also on the parasitic capacitance of the readout inductor. If the two elements of the telemetric system are fixed between the walls of the oven, the distance does not change and the sensor capacitance can be obtained from equation (2). Anyway, if the conditioning electronics is mounted over a mobile unit or the distance between the readout and hybrid sensor changes for any reason, the changing of the distance is compensated by the 3-Resonances method [18]. This method is based on a parameter, called "F", whose value depends only on distance.

$$F=(2\pi f_{ra})^2+(2\pi f_{rb})^2-(2\pi f_a)^2=\frac{1}{C_1\left(L_R+\frac{L_M L}{L_M+L}\right)} \quad (3)$$

If C_1 is fixed, "F" depends only on coupled and leakage fluxes: these values are related only to the distance and not to the transducer capacitance. Moreover, the parameter "F" is obtained by a direct measurement since it can be calculated by elaborating the measurement of the three f_{ra}, f_{rb} and f_a frequencies. Introducing the following expressions:

$$L=L_S\cdot n^2 \quad (4)$$

$$C=\frac{C'_S}{n^2} \quad (5)$$

$$L_1=L_R+L_M \quad (6)$$

$$L_2=L_S+\frac{L_M}{n^2} \quad (7)$$

Substituting equations (4), (5), (6) and (7) into (2) and in (3) and re-arranging the expressions, the ratio of equation (3) with equation (2) is equal to:

$$\frac{F}{(2\pi f_a)^2}=\frac{L_2 C'_S}{L_1 C_1} \quad (8)$$

Re-arranging (8), a straightforward expression of the sensor capacitance (C'_S) is:

$$C'_S=\frac{L_1 C_1}{L_2}\frac{F}{(2\pi f_a)^2} \quad (9)$$

C'$_S$ is obtained as a product between a constant term and a second one calculated from the three measured f_{ra}, f_{rb} and f_a frequencies. The constant term can be automatically obtained from a calibration operation or can be calculated measuring the equivalent circuit parameters of the each single planar inductor: L_1 and L_2 are the self-inductances of the read-out and sensing inductances, while C_1 is the parasitic capacitance (or any other added capacitance) of the readout circuit. The equivalent circuit parameters of every single inductor separately (consisting in the series of an inductance and a resistance both in parallel with a capacitance) have been measured by the impedance analyzer HP4194A and their values are reported in Table 1.

Inductors	*Inductance (μH)*	*Capacitance (pF)*	*Resistance (Ω)*
Sensing Inductor	235	1.8	80
Readout Inductor	14.5	91.4	22

Table 1. Equivalent circuit parameters.

IV. MEASUREMENT ELECTRONIC

As previously reported, to calculate $C's$, the measurement of the three resonant frequencies (f_{ra}, f_{rb}, f_a) is required. These are the resonance frequencies of Z_E and are frequency points whose phase is zero. The impedance measured to the readout terminals is Z'$_E$. Its diagram is reported in Figure 5, where is possible to individuate three points f'_{ra}, f'_a f'_{rb}, that corresponds, in succession from right to left to the first maximum and minimum respectively, while f'_{rb} is the second maximum. When the resistance components of the model (Figure 2) have zero value the three resonant frequencies f_{ra}, f_a f_{rb} and f'_{ra}, f'_a f'_{rb} respectively coincide. In the real case, the resistances of the readout inductor and of the hybrid sensor have about 22 Ω and 80 Ω at 25 °C respectively. Their values are also subjected to change with temperature. In this case f'_{ra}, f'_a does not coincide with f_{ra}, f_a. The error introduced in the calculation of C'_S using f'_{ra}, f'_a instead of f_{ra}, f_a have been estimated and it is reported in Figure 6 as a function of the resistance values. The data have been obtained from Spice simulation. Physical models of the readout inductor and hybrid sensor have been tune up from experimental measurement. The simulation results are show in Figure 6, where the values of f'_{ra}, f'_a are reported as a function of the resistance. The values of f_{ra}, f_a are 1.125 MHz and 1.179 MHz.

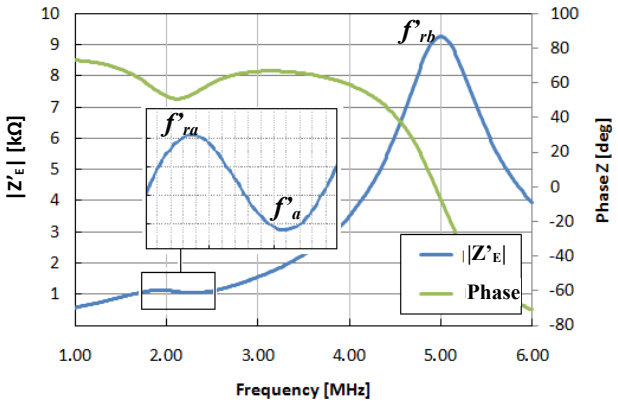

Fig. 5. Module and phase of the Z'$_E$ impedance.

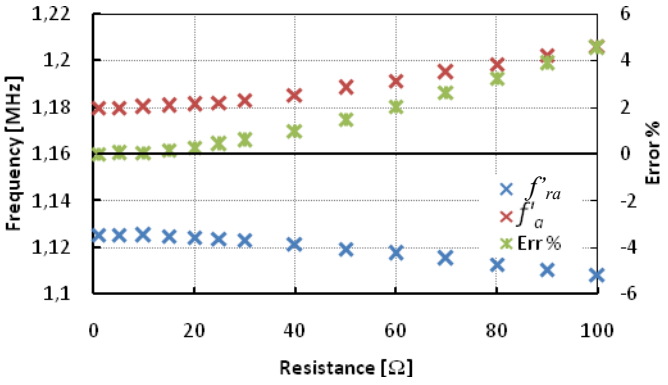

Fig. 6. Frequencies f'_{ra}, f'_{rb} values and the error in the calculation of C'_S as a function of the resistance.

Approximately the resistance values of the model representing the real system are 80 Ω and 22 Ω and,

considering the worst case the error is about 3%. The measurement electronics calculates f'_{ra}, f'_{rb}, f'_{a} values acquiring the direct value of the real and imaginary components of the admittance in a defined frequency range. Subsequently the modulus and phase of the impedance are mathematically calculated with classical formula and the values of the three resonant frequencies are identified: f'_{ra}, f'_{a}, are the first maximum and minimum respectively, while f'_{rb} is the second maximum. The output sampled signals ($\mathrm{Re}[Y'_E]$ and $\mathrm{Im}[Y'_E]$) of electronic circuit (Figure 4) is proportional to the admittance of the load, and they can be represented as:

$$Y'_E = A + JB \tag{10}$$

Where A is $\mathrm{Re}[Y'_E]$ and B is $\mathrm{Im}[Y'_E]$. The microcontroller implements the following equation to extract the module and phase of admittance:

$$|Y'_E| = \sqrt{\mathrm{Re}[Y'_E]^2 + \mathrm{Im}[Y'_E]^2} \tag{11}$$

$$Phase[Y'_E] = \arctan\frac{\mathrm{Im}[Y'_E]}{\mathrm{Re}[Y'_E]} \tag{12}$$

After this conversion can be extracted the module and phase of impedance:

$$|Z'_E| = \frac{1}{|Y'_E|} \tag{13}$$

$$Phase[Z'_E] = -Phase[Y'_E] \tag{14}$$

V. Experimental Setup

An experimental setup has been designed to test the measurement system at high temperatures. In Figure 7 a block diagram of the experimental setup is shown.

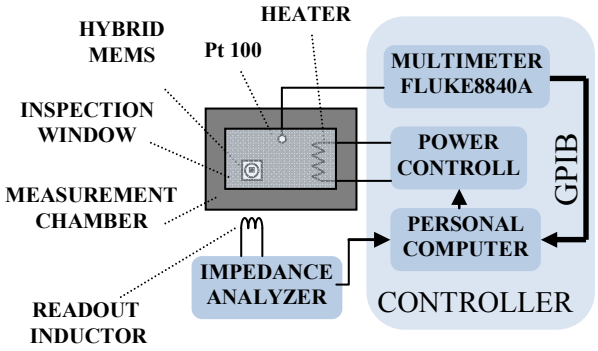

Fig. 7. Experimental setup for high temperature measurements.

The measurement chamber is isolated from the outside by two walls, one of aluminum and the other of steel; between them a thermo-resistive wool (Superwool607™ commercialized by Thermal Ceramics) is interposed. The total thickness of the measurement chamber is about 3 cm and the maximum space of the chamber is 30 cm x 30 cm x 13 cm. In one side there is a window of temperate glass, whose dimensions are12 x 12 cm, for visual inspection of the internal process. The maximum working temperature is about 500 °C. Inside the chamber an IR heater of 500 W controls the temperature. In order to assure that internal temperature is distributed uniformly, three thermo-resistances (Pt100) have been positioned in different points; each one is connected to a multimeter (Fluke 8840A). During the execution of the test, the maximum differences between the three thermoresistances have been about 0.2 Ω that corresponds to less than 1 °C. A personal computer, running a developed LabVIEW™ virtual-instrument, is connected to the multimeters through an IEEE 488 bus and to the input of the power control through the digital output of the I/O board. The PC monitors the temperature inside the oven and controls the IR-heater by turning on and off the power circuit. The hybrid sensor has been put inside the oven, while the readout inductor is placed outside at a distance of 1 cm from the sensor.

VI. Experimental Results

To test the telemetric measurement system the temperature inside the oven has been changed from about 50 °C to 330 °C with steps of 20 °C. Figure 8 and 9 show five profiles obtained interpolating the experimental data of respectively the module and phase of the Z'_E impedance in which two resonant frequencies (f'_{ra} and f'_{a}) are visible.

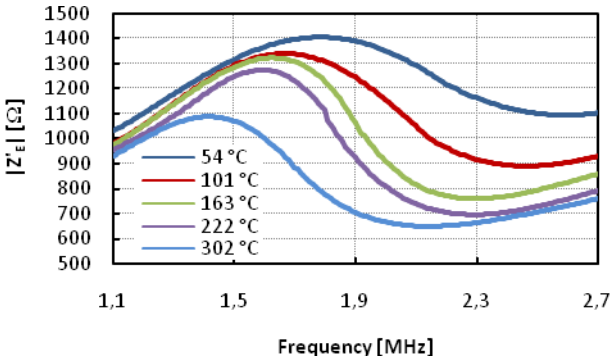

Fig. 8. Modulus of the hybrid MEMS measured with the impedance analyzer at different temperatures.

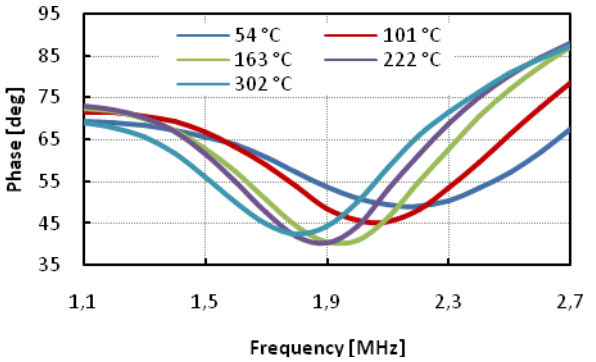

Fig. 9. Phases of the hybrid MEMS measured with the impedance analyzer at different temperatures.

From previous data shown in Figure 8 and Figure 9, the resonance frequencies have been identified as maximum and minimum points applying the 3-Resonance method, the values of the hybrid sensor capacitance has been calculated (equation 9). The constant term has been obtained by a calibration operation. Results are reported in Figure 10. In the graph below (Figure 10) the calculated capacitances are reported and are compared with the curve obtained from a direct measurement of the hybrid sensor capacitances using an impedance analyzer (HP4194A). The experimental data fit well the capacitance values obtained by a direct measurement.

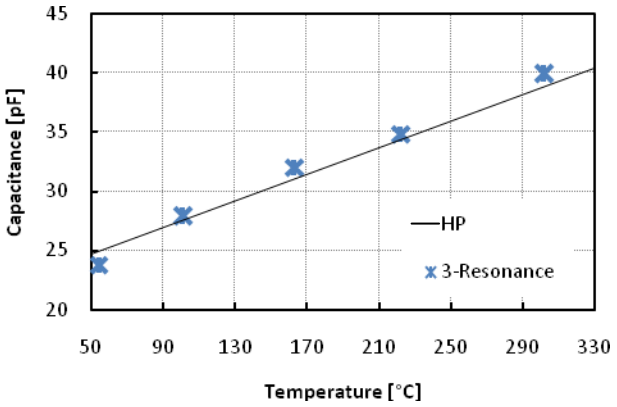

Fig. 10. Temperature compared with the impedance analyzer (HP4194A) measured capacitance and 3-Resonances capacitance calculated values.

VII. CONCLUSIONS

This work describes a system for measuring high temperatures in harsh environments. The system consists of a sensor placed in the measuring chamber and an external reading unit placed outside the measuring chamber in a "safe place". The sensor consists of a capacitive temperature transducer and a thick film inductor and measures temperature up to 330 °C. The reading unit can be fixed or mobile and can operate up to distances of few centimeters. The change of distance of readout unit can be compensated by the measurement technique used. The system was tested in the laboratory showing good agreement with reference data.

ACKNOWLEDGMENT

The Authors would like to acknowledge the staff guided by Prof. Baglio, University of Catania, for the support and the technical design of the MEMS. The authors wish to thank Marco Gazzoli for the support in the experimental phase.

REFERENCES

[1] M.V.P. Kruger, M.H. Guddal, R. Belikov, A. Bhatnagar, O. Solgaard, C. Spanos, K. Poolla, "Low Power Wireless Readout of Autonomous Sensor Wafer using MEMS Grating Light Modulator", Optical MEMS, 2000 IEEE/LEOS Int. Conf., 67-68.

[2] S.F. Lord, S.L. Firebaugh, A.N. Smith, "Remote Measurement of Temperature in the Presence of a Strong Magnetic Field", IEEE Transactions on Instrumentation and Measurement, 58, 2009, 674-680.

[3] J. Rodriguez, J. Meca, J.A. Jimenez, E.J. Bueno, "Monitoring and Quality Improvement of Pharmaceutical Glass Container's Manufacturing Process", IEEE Transactions on Instrumentation and Measurement, 57, 2008, 584-590.

[4] C. Beaucamp-Ricard, L. Dubois, S. Vaucher, P.Y. Cresson, T. Lasri, J. Pribetich, "Temperature Measurement by Microwave Radiometry: Application to Microwave Sintering", IEEE Transactions on Instrumentation and Measurement, 58, 2009, 1712-1719.

[5] D. Mavrudieva, J.Y. Voyant, A. Kedous-Lebouc, J.P. Yonnet, "Magnetic structures for contactless temperature sensor", Sensors and Actuators A 142, 2008, 464–467.

[6] J.W. Mrosk, L. Berger, C. Ettl, H.J. Fecht, G. Fischerauer, A. Dommann, "Materials Issues of SAW Sensors for High-Temperature Applications", IEEE Transactions On Industrial Electronics, 48(2), 2001, 258-264.

[7] M. R. Werner, W. R. Fahrner, "Review on Materials, Microsensors, Systems, and Devices for High-Temperature and Harsh-Environment Applications", IEEE Transactions on Industrial Electronics, 48(2), 2001, 249-257.

[8] M.A. Fonseca, M.G. Allen, J. Kroh, J. White, "Flexible Wireless Passive Pressure Sensors for Biomedical Applications", Tech. Dig. Solid State Sensor, Actuator, and Microsystems Workshop, Hilton Head Island, SC, USA, June 2006, 37-42.

[9] Y. Jia, K. Sun, F.J. Agosto, M.T. Quinones, "Design and characterization of a passive wireless strain sensor", Measurement Science and Technology 17, 2006, 2869–2876.

[10] E. Birdsell, M. G. Allen, "Wireless Chemical Sensors for High Temperature environments", Tech. Dig. Solid-State Sensor, Actuator, and Microsystems Workshop, Hilton Head Island, SC, USA, June 2006, pp. 212-215.

[11] E.L. Tan, W.N. Ng, R. Shao, B.D. Pereles, K.G. Ong, "A Wireless, Passive Sensor for Quantifying Packaged Food Quality", Sensors 7, 2007, 1747-1756.

[12] Y. Wang, Y. Jia, Q. Chen, Y. Wang, "A Passive Wireless Temperature Sensor for Harsh Environment Applications", Sensors 8, 2008, 7982-7995.

[13] L.A. Barragan, D. Navarro, J. Acero, I. Urriza, J.M. Burdío, "FPGA Implementation of a Switching Frequency Modulation Circuit for EMI Reduction in Resonant Inverters for Induction Heating Appliances", IEEE Transactions on Industrial Electronics, 55(1), 2008, 11-20.

[14] J. Qin, C.E. Stroud, F. F. Dai, "FPGA-Based Analog Functional Measurements for Adaptive Control in Mixed-Signal Systems", IEEE Transactions on Industrial Electronics, 54(4), 2007, 1885-1897.

[15] A.O. Niedermayer, T. Voglhuber-Brunnmaier, E.K. Reichel, B. Jakoby, "Improving the Precision of a Compact Subsampling Impedance Analyzer for Resonating Sensors", Proceedings of the Eurosensors XXIII conference, Procedia Chemistry 1, 2009, 1335–1338.

[16] J.S. Riquelme, F.S. Quijano, A. Baldi, M.T. Oses, Low power impedance measurement integrated circuit for sensor applications, Microelectronics Journal 40, 2009, 177-184.

[17] J. Castelló, R. García-Gil, J.M. Espí, "A PC-based low cost impedance and gain-phase analyzer", Measurement 41, 2008, 65–75.

[18] D. Marioli, E. Sardini, M. Serpelloni, B. Andò, S. Baglio, N. Savalli, C. Trigona, "Hybrid Telemetric MEMS for High Temperature Measurements into Harsh Industrial Environments", Proceedings of I2MTC 2009, Singapore, 2009, 1423-1428.

[19] B. Andò, S. Baglio, N. Pitrone, N. Savalli, C. Trigona, "Bent beam MEMS Temperature Sensors for Contactless Measurements in Harsh Environments", Proceedings of IEEE I2MTC 2008, Victoria, BC, Canada, 2008, 1930-1934.